Talanta 101 (2012) 135–140

Contents lists available at SciVerse ScienceDirect

Talanta

journal homepage: www.elsevier.com/locate/talanta

Graphene in combination with cucurbit[*n*]urils as electrode modifiers for electroanalytical biomolecules sensing

Mireia Buaki-Sogo [a], María del Pozo [b], Pedro Hernández [b], Hermenegildo García [a], Carmen Quintana [b,*]

[a] Instituto Universitario de Tecnología Química CSIC-UPV and Departamento de Química, Universidad Politécnica de Valencia, 46022 Valencia, Spain
[b] Departamento de Química Analítica y Análisis Instrumental, Universidad Autónoma de Madrid, Cantoblanco, 28049 Madrid, Spain

ARTICLE INFO

Article history:
Received 7 May 2012
Received in revised form
27 August 2012
Accepted 3 September 2012
Available online 18 September 2012

Keywords:
Graphene
Cucurbit[*n*]uril
Electrochemical sensors
Supramolecular interactions
Biomolecules sensing

ABSTRACT

Cucurbit[*n*]urils have been supported on graphene to develop sensitive and selective electrodes. The electrochemical response of modified electrodes containing graphene or graphene plus cucurbiturils has been studied for three probe molecules including hydroxymethylferrocene, ferrocyanide and methylviologen. It was found that the properties of these modified electrodes are derived from an increase in electron mobility and catalytic activity imparted by graphene and the selective complexation and molecular recognition due to cucurbit[*n*]urils. These properties of the graphene/cucurbit[*n*]urils modified electrodes have been applied for the electrochemical detection of relevant biomolecules as tryptophan at 0.69×10^{-7} M concentration.

1. Introduction

Carbon based materials, from classical carbon paste or glassy carbon, to more recently employed carbon nanotubes, have been widely used in electrochemical applications [1]. Nowadays, the availability of graphene and their unique properties in terms of electron mobility is attracting considerable attention for its use in electrochemistry [2]. Therefore, a great number of papers related to the fundamentals, properties and applications of graphene, including sensing, electrocatalysis and electronics [3–5], can be found in recent literature [6].

Different electrochemical sensors based on graphene and graphene composites have been previously reported for biosensor development [1,7] and for the detection of small biomolecules including ascorbic acid [8] or dopamine [2,9,10], allowing the simultaneous determination of both with different graphene-based modified electrodes.

Some authors have tried to avoid the trend of graphene nanosheets to form agglomerates or even restack to graphite by using cyclodextrins (CDs) as additives for the preparation of stable aqueous suspensions of graphene nanosheets [11] or as dispersive agents in a β-CD/graphene nanocomposite platform for dopamine nanomolar detection [10]. This strategy has opened the possibility of combining the graphene electrical properties with molecular recognition of CDs either in graphene/CDs or graphene/CDs/metal nanoparticles composites, and these electrodes have been applied with excellent performance to the selective and high sensitive determination (at nM level) of different analytes with relevance in biological, clinical or environmental fields [12–14]. All these works have contributed to the design of more complex supramolecular nanostructures built from multifunctional components through non-covalent interactions [15].

The recent availability cucurbit[*n*]urils (CB[*n*]s; $n=5$–8, 10) and the strong binding constants of some of their inclusion complexes has motivated the interest in the exploitation of these interesting host–guest complexes in various fields. CB[*n*]s are cyclic organic capsules with a pumpkin like shape with a hydrophobic inner cavity that is accessible through two portals with polar carbonyl groups which confers them their host–guest properties. In addition, the negative charge density located at the carbonyl groups, allows the stabilization of inclusion complexes with positively charged guests by ion-dipole and hydrogen-bonding interactions. In contrast to CDs, this circumstance allows the possibility of CB[*n*]s interactions with metals or positive ions leading to the formation of strong adducts. The unique interaction possibilities offered by these interesting macrocycles make them excellent candidates to be used in chemical sensor development. Compared to CDs, CBs have stronger binding constants in aqueous medium that could lead to a higher selectivity.

Considering that the larger dimensions of CB [8] make this capsule a suitable host for a wide range of organic molecules and its low water solubility (<0.01 mM), CB [8] is among the best candidates as an electrode modifier. To the best of our knowledge,

* Corresponding author. Tel.: +34 914977626; fax: +34 914974931.
E-mail address: carmen.quintana@uam.es (C. Quintana).

0039-9140/$ - see front matter © 2012 Elsevier B.V. All rights reserved.
http://dx.doi.org/10.1016/j.talanta.2012.09.016

no attempts to explore the effect of CBs on the graphene properties have been reported in the literature. Herein we present the preparation and electrochemical performance of a graphene containing CB[*n*]s (*n*=7 and 8) with new supramolecular recognition capabilities which showed promising results as selective electrochemical sensor.

The incorporation of CB[*n*] on the electrode surface was expected to increase the selectivity of the electrode surface as these macrocyclic receptors have proved their ability for form selective host–guest complexes diminishing interferences of negatively-charged analytes in a sample mixture [16,17]. The selection mechanism of these compounds based on formation of host–guest complexes leads generally to a significant decrease in the electrochemical signal of the target analyte. One possibility to circumvent this problem is to embed these capsules inside a conductive carbon matrix and, therefore, we anticipate that the combination of CB[*n*]s with graphene should result in a good choice to develop selective and sensitive electrodes in which each component offsets the limitation of the other and introduce the desirable property of selectivity (CB [8]) and sensitivity (graphene).

2. Experimental

2.1. Reagents

Graphite, cucurbit [7,8]uril, L-tryptophan (Try) (98%), dopamine (Dp), hydroxymethylferrocene (FcOH), potassium ferro/ferricyanide ($K_3[Fe(CN)_6]$/ $K_4[Fe(CN)_6]$) and methylviologen dichloride hydrate (MV^{2+}) were obtained from Sigma-Aldrich Chemical Co. (St. Louis, USA). L-tyrosine (> 99%), L-cysteine (99%), D-phenylalanine (98%), lysine (> 98%) and arginine (> 99%) were purchased from Sigma-Aldrich Chemical Co. (St. Louis, USA).

All reagents used were of analytical reagent grade. Solvents were purchased from Scharlau (Barcelona, Spain), and Milli-*Q* water was purified with a Milli Ro Milli *Q* Plus 185 apparatus from Millipore (Waters, Milford, USA).

2.2. Apparatus

Electrochemical measurements were carried out with a μ-Autolab potenciostat (Type III and Gpes software from Eco-Chemie, Utrech, The Netherlands). A conventional three-electrode system was used with a glassy carbon electrode (GC) of 3 mm in surface diameter as a working electrode to be modified (either with graphene, GC/G, or with graphene/CB[*n*], GC/G–CB[*n*]). Ag/AgCl/KCl (3 M) was used as a reference electrode and a coiled platinum wire as counter one. An 827 pH lab pH-meter from Metrohm (Herisau, Switzerland) was employed for buffer solutions preparation.

Impedance measurements were performed with a Frequency Response Analyzer (FRAII) from Eco-Chemie (Utrecht, The Netherlands, www.ecochemie.nl) coupled with the potentiostat.

Elemental analysis was performed in a FISONS EA 1108 CHNO-S analyser and Raman spectra were acquired in a Renishaw Invia Raman Microscopy system using a 514.5 nm (15 or 30 mW) diode aircooling laser (Reinshaw HPNIR) with a Peltier charge-coupled device (CCD) as a detector. Transmission electron microscopy (TEM) images were acquired with a Philips CM300 FEG system with an operating voltage of 100 kV.

2.3. Procedure

2.3.1. Preparation of G and G–CB[n]s

The preparation of G and G/CB samples for electrode modification was carried out by the reduction, in the presence or the absence of CBs, of a graphene oxide suspension. Hydrophilic GO was synthesized by chemical oxidation of graphite according to Hummers method [18]. Graphite flakes (3 g) were suspended in a mixture of concentrated H_2SO_4/H_3PO_4 (360:40 ml). To this mixture, $KMnO_4$ (18 g) was added producing an exothermic reaction that raises the temperature that has to be maintained in the range of 35–40 °C by cooling. Once the addition of $KMnO_4$ is complete, the suspension is stirred for 30 min and then heated to 50 °C under magnetic stirring for 12 h. The reaction was cooled to room temperature and poured into 400 g of ice containing 30% H_2O_2 (3 ml) and allowed to react for 4 h. After this time, the suspension was filtered, and the solid washed with a 1:10 HCl (37%) solution and then further with water. Then 50 mg of this solid were exfoliated by sonication in Milli-*Q* water (300 ml) for 2 h with an ultrasound source (400 W) to get an aqueous suspension of individual GO sheets with a concentration of 167 mg/l. The graphene sample not containing CB was obtained by the reduction of graphene oxide suspension (100 ml, 0.167 mg/ml), under nitrogen atmosphere, using hydrazine (70 μl). The mixture was stirred at 100 °C for 24 h. For the samples containing CBs, the preparation was carried out as follows: to the suspension of graphene oxide (100 ml, 0.167 mg/ml), 20 mg of the corresponding CB[*n*] (*n*=7, 8) were added and the mixture was sonicated for 5 min and then stirred at 40 °C for 30 min under nitrogen atmosphere. Then, 70 μl of hydrazine were added and the solution stirred at 100 °C for 24 h. After this time, for both G and G–CB samples, the suspension was centrifugated at 9000 rpm for 15 min and the supernatant was removed. The remaining solid was washed with Milli-*Q* water (10 ml) followed centrifugation at 9000 rpm for 15 min and the cycle washing/centrifugation repeated for a second time. The residue collected from the centrifuge tube was finally submitted to liophilization to obtain a dry sample that was used for electrode preparation.

2.3.2. Electrode modification

The hybrid electrode surfaces were prepared as follows: G–CB[*n*] (*n*=7/8) suspensions (0.3 mg/ml) in ultrapure water were sonicated for 30 min to get a high homogenized dispersion. Next, an aliquot of 10 μl was dropped on a freshly polished GC electrode surface and let to dry at ca. 40 °C for 30 min. For comparison, the same procedure was carried out with graphene suspensions in water. Before each modification, the GC electrode was polished with 0.3 μm alumina slurry for 1 min on a polishing cloth, rinsed with ultrapure water and sonicated consecutively in ethanol (30 s) and deionized water (30 s) for three times to remove any residual polishing material before being dried under nitrogen flow [19]. The electrode was then cycled between −0.2 and 1.3 V in supporting electrolyte until a reproducible signal was obtained.

2.3.3. Electrochemical measurements

Cyclic voltammograms were carried out scanning the potential at 100 mV/s in 0.1 M phosphate buffer pH=7.00 ± 0.01 with different probes at 1×10^{-3} M concentration level. Differential pulse measurements were recorded from Try solutions after 150 s of accumulation at 0.3 V, in the range of 0.3–1.2 V, with a pulse amplitude of 80 mV and a scan rate of 30 mV/s in steps of 15 mV and an interval time of 0.5 s.

Impedance measurements were performed in a 0.1 M phosphate buffer pH=7.00 ± 0.01 with 1×10^{-3} M $K_3[Fe(CN)_6]$/ $K_4[Fe(CN)_6]$ solutions at the equilibrium potential. Measurements were taken in the frequency range of 0.1 Hz to 0.1 MHz with a sinusoidal voltage amplitude of 5 mV. The experimental data were plotted in the form of Nyquist plots.

2.3.4. Sample preparation

Sample preparation procedures were similar to other previously described for Try analysis in serum [16,20] and pharmaceutical formulation samples [21]. Briefly, human blood was centrifuged during 10 min at 2500 rpm and 4 °C. Next, the serum was separated with a syringe and frozen until it was analysed. Serum samples were deproteinized by addition of 5% (v/v) of perchloric acid. After refrigeration overnight, samples were centrifuged at 6000 rpm for 10 min.

Pharmaceutical formulation samples (tablets for human consumption, El Reco, 400 mg Try per tablet) were prepared as follows: The weight of one tablet (581 mg) was calculated from the average of 20 tablets. An accurate amount of about 10 mg of the sample was dissolved in methanol/water (50/50, v/v). The solution was sonicated, filtered through a 0.45 μm nylon filter and diluted with methanol/water (50/50, v/v) in a volumetric flask up to a 50 ml.

3. Results and discussion.

3.1. G–CB samples characterization.

Graphene oxide was obtained by Hummers oxidation of graphite [18] followed by exfoliation in water. The degree of oxidation was determined by chemical analyses of the dry graphene oxide powder after water evaporation and drying, giving 37.38 wt % of C content, the rest being oxygen. The aqueous solution of graphene oxide (0.167 mg/ml) was reduced with hydrazine at 100 °C to form reconstituted G that was used as electrode modifier immediately after its preparation. When required, the solutions containing graphene oxide were saturated with CB[*n*] (*n*=7 or 8), 20 mg, that were dispersed in the reconstituted graphene suspension by sonication.

The samples of G–CB were characterized by Raman spectroscopy where the characteristic D and G bands of graphene-like materials appearing at 1353 and 1594 cm^{-1} were observed (see Fig. S1). No peaks corresponding to CB were detected by Raman spectroscopy, this being in accordance with the low proportion of this organic capsule and the more intense Raman of graphene. On the contrary, as shown in Table 1, elemental analysis of the G–CB materials prepared allowed us to confirm that the macrocyclic receptors were successfully incorporated as can be deduced from the presence of nitrogen in more than 12 and 14% amount which, respectively, represent a 66 and 78% of the initial CB [7] and CB [8] added.

Table 1
Elemental data analysis.

	%N	%C	%H
Graphene	0.100	73.198	1.230
Graphene@CB [7]	12.192	61.051	2.564
Graphene@CB [8]	14.310	48.971	2.625

For electrode modification, a few microlitres of aqueous suspensions of these materials were deposited on a freshly polished GC electrode and the water allowed evaporating at 40 °C.

TEM images of the dry G–CB sample used for electrode modification are shown in Fig. 1 at two different magnifications. Only the characteristic graphene features are observed, the sample being constituted by sheets of about 10 μm size, relatively free of amorphous carbon debris. The wrinkles observed at higher magnification are indicative of flexible, single-sheet graphene material. The fact that the presence of CBs cannot be inferred from the TEM images is compatible with these organic capsules being well dispersed on the graphene layer.

3.2. Electrochemical characterization

Cyclic voltammetry and electrochemical impedance spectroscopy techniques have been employed to test the presence of the macrocyclic receptor in the materials and the possibility of their application as selective electrochemical sensors. To this end and, taking into account the known ability of CB[*n*]s to form inclusion complexes, different compounds have been chosen as electrochemical probes. Therefore, 1×10^{-3} M individual solutions of FcOH, MV^{2+} or $Fe(CN)_6^{3-}$/ $Fe(CN)_6^{4-}$ were studied employing the modified electrodes described above.

As is shown in Fig. 2, a great increase in the current intensity respect to that obtained with the bare electrode is produced when G is used as electroactive surface. The presence of CB [7] and CB [8] in the corresponding graphene materials can be concluded from the decrease in the signal intensities, more accused when working with CB [7] homologue [22], and from a slight deviation from the probe

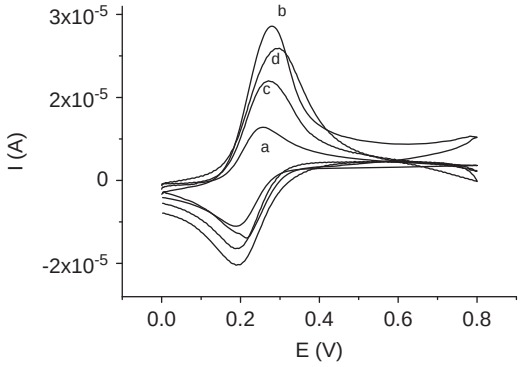

Fig. 2. Cyclic voltammograms of 1×10^{-3} M FcOH solutions recorded with different modified electrodes. (a) Bare GC, (b) GC/G, (c) GC/G–CB [7] and (d) GC/G–CB [8]. V_b=100 mV/s.

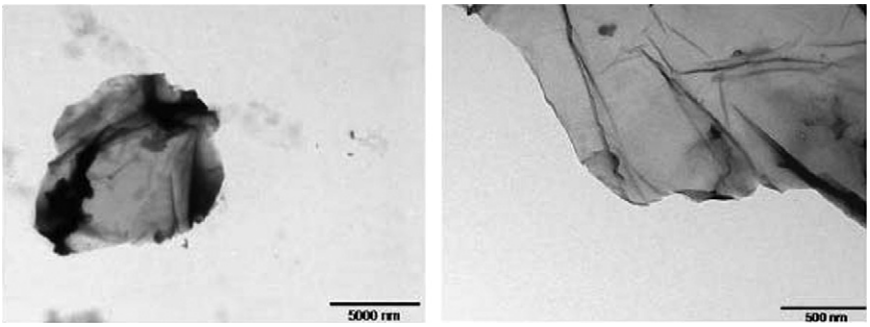

Fig. 1. TEM images of dry G–CB [8] sample used for electrode modification.

reversible electrochemical behavior as is shown by the calculated ΔE_{a-c} values that ranged from 59 mV working with the bare GC electrode to 98 mV for the GC/C-CB[8]. Table 2 compiles the ΔE_{a-c} values and the relative intensity of the anodic vs. cathodic peaks.

The semicircle observed at high frequencies values in the Nyquist plots recorded from electrochemical impedance measurements is related to the charge-transfer limiting processes. As shown in Fig. 3A, the graphene-modified electrodes facilitates the charge transfer as no clear semicircle can be observed in the corresponding plots. For these electrodes containing G, a fast electrochemical process with lower charge-transfer resistance is observed according to the cyclic voltammograms depicted in Fig. 3B.

As stated in introduction section, CBs can stabilize inclusion complexes with positively charged guest fitting with their size. The voltammetric behaviour of MV^{2+} shows two reversible waves corresponding to the redox pairs $MV^{2+}/MV^{+\cdot}$ and $MV^{+\cdot}/MV^{0}$. The use of MV^{2+} as probe is suitable for CB [8] on the graphene-based material as this guest shows the first redox couple pair at less negative potentials respect to the free MV^{2+}, corresponding to the formation of the CB [8]/MV^{2+} complex and its easier reduction [23].

The voltammograms depicted in Fig. 4A, corresponds to MV^{2+} solutions recorded with the bare GC, GC/G and the GC/G–CB[8] electrodes. Only in this last case, it was possible to observe a second redox pair that is attributed to the first redox process of the CB [8]/MV^{2+} complex reduction providing experimental evidence of the formation of this host–guest complex on the electrode surface. To confirm that we are measuring the complex on the electrode surface, we scanned the potential between −0.3 and −0.9 V in a supporting electrolyte solution after having immersed the GC/C–CB [8] modified electrode in a 1×10^{-3} M MV^{2+} solution for 5 min under constant stirring. The results are depicted in Fig. 4B where a small signal can be observed only when the electrode is modified with G/CB [8].

As graphene-based electrochemical sensors have recently shown very good analytical properties for the detection of biomolecules such as Dp [10,24] or Try [25] and, as there is known the interactions of these guests with CB [8], we tested the performance of graphene-modified electrodes containing or not CB [8] for the sensing of these analytes. As can be observed in Fig. 5, in addition to the Dp peak current increase, a shift of the Dp peak potential to less positive values is observed with the GC/G modified electrode showing a more reversible electrochemical behaviour (ΔE_{a-c} values of 181 and 65 mV for the bare and GC/G electrode, respectively). The results obtained working with the GC/G–CB [8] modified electrode (voltammogram c) demonstrate again, not only the electrocatalytic activity of graphene but also that the host–guest CB [8] interaction capability is maintained in the electrode developed.

Try shows higher oxidation overpotential and relative low electroactivity in comparison with Dp. Moreover, the affinity of this relevant amino acid for the CB [8] cavity has been employed in different applications [16,26,27]. Therefore, the combination of both, graphene and CB [8], the lowest soluble CB[*n*] homologue, is worthy to be explored.

The results depicted in Fig. 6 confirm the expectancy about the benefits of using graphene-containing CBs as an electrochemical sensor. Lower overpotentials are required for Try oxidation and the peak current increases 2.9 times with GC/G electrode respect to that recorded with the bare one. The complex formation can be deduced from the shift of the peak potential to more positive values respect GC/C although still lower than that with the GC. As a result of combining both, graphene and CB [8], lower oxidation potential with an increase in the peak current up to 1.8 fold respect to the unmodified electrode can be obtained. After 150 s of accumulation at the initial potential, square wave voltammograms of increasing Try concentrations showed a linear increase in the *Ip* in the 1.12×10^{-7} to 3.00×10^{-6} M range according to the equation $Ip\ (A)=(-5.6\pm1.8)\times10^{-8}+(1.57\pm0.01)$ [Try] (M) ($r=0.9996$). The detection and quantification limits (calculated as 3*s*/slope and 10*s*/slope, where *s* is the mean value of three blank voltammograms) were 0.69×10^{-7} M and 1.48×10^{-7} M, respectively. These values are slight better than those previously reported by our group employing Nafion/CB [8] modified electrode [16] or even better than others previously reported using graphene-based modified electrodes [25].

The accuracy and precision of the proposed method were evaluated at three different concentrations in the linear response range (3.00×10^{-7}, 4.00×10^{-7}, 8.09×10^{-7} and 3.09×10^{-6} M). RSD $(\%)_{n=3}$ values of 7.7%, 5.9%, 3.8% and 3.3% were calculated for each concentration assayed. The calculated *Er* values (corresponding at the concentration levels stated above) were 6.7%, 1.9%, 3.8% and 3.3%, respectively.

Reproducibility corresponding to different modified surfaces was evaluated at the same four concentration levels and the RSD $(\%)_{n=5}$ values 2.0% (4.00×10^{-7} M) to 13% for the highest concentration assayed. Finally, stability of the modified surface was also tested by measuring a Try solution (8.09×10^{-7} M) during successive days. The reproducibility of the signal was better than 15% during 11 days. After that, a noticeable decrease in the signal was recorded.

Table 2
Evolution of the characteristic cyclic voltammetric FcOH parameters as result of the different modifications.

	Bare GC	GC/G	GC/C–CB [7]	GC/C–CB [8]
ΔE_{a-c} (mV)	59	61	76	98
Ip_a/Ip_c	1.20	2.46	1.50	1.73

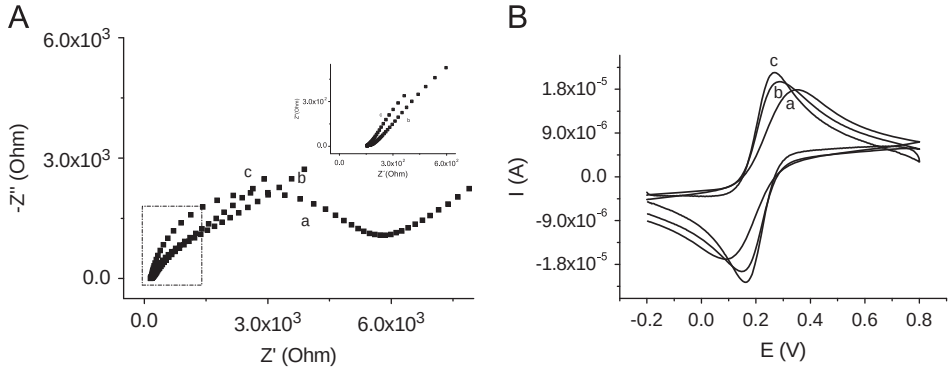

Fig. 3. (A) Nyquist plots of 1×10^{-3} M $FeCN^{3-}/^{4}$ solutions recorded with different modified electrodes. (a) Bare GC, (b) GC/G, (c) GC/G–CB [8]. (B) Cyclic voltammograms of 1×10^{-3} M $FeCN^{3-}/^{4}$ solutions recorded with different modified electrodes. $V_b=100$ mV/s.

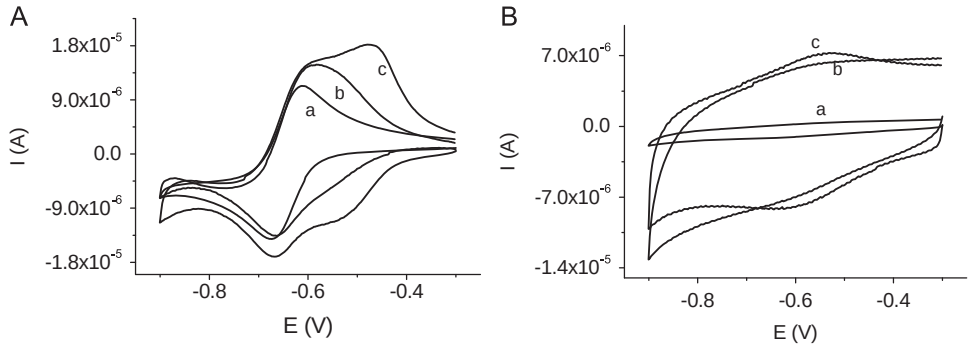

Fig. 4. (A) Cyclic voltammograms of 1×10^{-3} M MV^{2+} solutions recorded with different modified electrodes. (B) Cyclic voltammograms recorded in supporting electrolyte after immersing the different electrodes in a 1×10^{-3} M MV^{2+} solution. (a) Bare GC, (b) GC/G, (c) GC/G–CB [8]. V_b=100 mV/s, 0.1 M phosphate buffer, pH=7.00 ± 0.01.

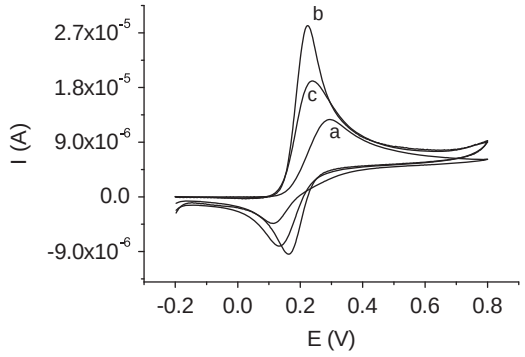

Fig. 5. Cyclic voltammograms of 1×10^{-3} M Dp solutions recorded with different modified electrodes. (a) Bare GC, (b) GC/G, (c) GC/G–CB [8]. V_b=100 mV/s, 0.1 M phosphate buffer, pH=7.00 ± 0.01.

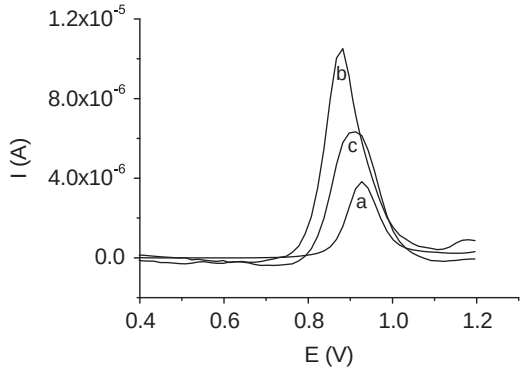

Fig. 6. Differential voltammograms of M Try solutions recorded with different modified electrodes. (a) Bare GC, (b) GC/G, (c) GC/G–CB[8]. V_b=100 mV/s, 0.1 M phosphate buffer, pH=2.00 ± 0.01.

3.2.1. Interference studies

In order to study the capability of discrimination of the developed sensor, different amino acids were evaluated as potential interferences in the Try determination. L-tyrosine (L-Tyr), L-cysteine (L-Cys), D-phenylalanine (D-Phe), lysine (Lys) and arginine (Arg) were selected for this purpose. Thus, increasing amounts of the target compounds were added to a Try solution at 8.09×10^{-7} M concentration level. To perform the study, it was considered that a substance produces interference at a concentration level that leads to a variation equal of higher than the maximum *Er*% of the method.

Among all the compounds tested, only L-Tyr presents an oxidation peak under the experimental conditions, almost at same potential as Try. However, up to two-fold Tyr concentration in solution respect to Try is allowed without producing interference. On the contrary, the presence of Lys up to 8.11×10^{-5} M (100 fold Lys/Try concentration ratio) does not produce any significant variation in the Try peak current (0.6%). As Lys, no electrochemical signals under the experimental conditions were recorded for the rest of amino acids assayed. However, their presence in solution modifies the Try peak current to some extent. In all these cases, higher interference/Try concentration ratios are needed to produce interference. So, the presence of D-Phen or L-Cys are allowed up to 2.83×10^{-5} M and 4.04×10^{-5} M concentration levels, respectively (35 and 50 fold D-Phen/Try and L-Cys/Try concentration ratios), while Arg would not produce interference up to 1.05×10^{-6} M under the criterion selected.

3.2.2. Analytical application

The performance of the proposed methodology was tested for the analysis of Try in two different real samples: human serum samples and pharmaceutical formulations. In both cases, the standard addition method was employed for quantification.

3.2.2.1. Serum samples. A volume of 0.5 ml of unfortified serum subsamples (i.e., non-spiked samples) and fortified at five different concentration levels ranging from 0.59 to 2.94 μM (all of them treated as described in Section 2.3.4) were diluted to 10 ml in a supporting electrolyte. These latter solutions were set in the electrochemical cell and the corresponding differential pulse voltammograms were recorded. A linear increase in the peak intensity current with increasing Try amounts were observed according to $Ip(A)=(1.05 \pm 0.30) \times 10^{-7}+(0.37 \pm 0.02)$ [Try] (M), r=0.992; thus giving a calculated Try concentration of (42.2 ± 4.0) μM (n=3). These results are similar to other previously reported when analyzing healthy human serum samples [20]. An RSD value of 9.5%, obtained as a result of the three analyses carried out, and recoveries ranging from 71 to 108% (see Table 3) show that the proposed methodology can be applied with enough accurate and precision.

3.2.2.2. Pharmaceutical formulations. In this case, a subsample of 40 μl (treated as described in Section 2.3.4) was diluted to 25 ml with a supporting electrolyte and the corresponding differential pulse voltammograms were recorded. This procedure was applied to non-spiked subsamples and to different 40 μl subsamples spiked with increasing Try amount in the range of 0.29–2.65 μM. In this case, the increase in the peak intensity current with Try concentration was fitted to Ip (A)$=(8.7 \pm 0.5) \times 10^{-7}+(0.73 \pm 0.03)$ [Try] (M), r=0.996. From these data, an average Try value of (379 ± 23) mg per tablet (n=3) was obtained. A good agreement between the Try reported by the manufacturer (400 mg/tablet) and the Try found was obtained. Thus, an *Er*=5% as average of the three determinations and an RSD value of 6.1% were obtained.

Table 3
Recovery values obtained for the Try determination in real samples.

Sample	$[TRP]_{added}$ (μM)	Recovery (%)
	0.59	106
	1.18	71
Human serum	1.76	93
	2.35	98
	2.94	108
	0.29	90
	0.88	96
Pharmaceutical formulation	1.47	94
	2.06	105
	2.65	105

Recovery results corresponding to both samples are summarized in Table 3, showing that the method can be successively applied to the analysis of Try in different matrices.

4. Conclusions

Herein we have shown that modified electrodes based on graphene and CB[*n*]s combine the high electron mobility and catalytic activity imparted by graphene with the selective binding and molecular recognition by formation of inclusion complexes with CB[*n*]s. In this way, the electrochemical response of these modified electrodes is significantly higher than that measured under identical conditions by bare glassy carbon electrodes, with an enhancement of the oxidation anodic peaks, due to the presence of graphene. In addition, there are some remarkable shifts in the peak potentials when the probe is able to form an inclusion complex with CB. The combination of this enhanced electrochemical response with selective binding is of interest for the development of electrochemical sensors and has been exemplified with the results observed for two favorite biomolecules, namely, dopamine and tryptophan. Moreover, the performance of this electrochemical sensor has been proved applying it to the analysis of Try in different real samples with enough accurate and precision. To the best of our knowledge, this is the first time in which CB[*n*]s have been incorporated in reconstituted graphene to develop electrochemical sensors and opens the way to a new generation of modified graphene materials obtained by functionalization of graphene oxide that combines sensitivity and selectivity as selective electrodes.

Acknowledgements

Financial support by the Spanish Ministry of Economy and Competitiveness (CTQ2009-11856 and CTQ2007-67805/PPQ), the Comunidad Autónoma de Madrid (S2009/PPQ-1642, AVANSENS) and the Ministry of Science and Innovation (CTQ2008-02272/PPQ) is gratefully acknowledged. M. del Pozo thanks the Ministry of Science and Innovation for a PhD grant.

Appendix A. Supporting information

Supplementary data associated with this article can be found in the online version at http://dx.doi.org/10.1016/j.talanta.2012.09.016.

References

[1] J. Wang, Electroanalysis 17 (2005) 7–14.
[2] Y. Shao, J. Wang, H. Wu, J. Liu, I.A. Aksay, Y. Lin, Electroanalysis 22 (2010) 1027–1036.
[3] Z. Wang, J. Zhang, P. Chen, X. Zhou, Y. Yang, S. Wu, L. Niu, Y. Han, L.a.C. Wang Peng, F. Boey, Q. Zhang, B.a.Z. Liedberg Hua, Biosens. Bioelectron. 26 (2011) 3881–3886.
[4] D. Han, T. Han, C. Shan, A.a.N. Ivaska Li, Electroanalysis 22 (2010) 2001–2008.
[5] J.Q. Liu, Z.Y. Yin, X.H. Cao, F. Zhao, A.P. Lin, L.H. Xie, Q.L. Fan, F. Boey, H. Zhang, W. Huang, Acs Nano. 4 (2010) 3987–3992.
[6] D.A.C. Brownson, C.E. Banks, Analyst 135 (2010) 2768–2778.
[7] X. Chen, H. Ye, W. Wang, B. Qui, Z. Lin, G. Chen, Electroanalysis 22 (2010) 2347–2352.
[8] D.V. Stergiou, E.K. Diamanti, D. Gournis, M.I. Prodromidis, Electrochem. Commun. 12 (2010) 1307–1309.
[9] Y. Kim, S. Bong, Y. Kang, Yang, Yongtak, Mahajan, Rakesh Kumar, J.S. Kim, H. Kim, Biosens. Bioelectron. 25 (2010) 2366–2369.
[10] L. Tan, K. Zhou, Y. Zhang, H.a.W Wang Xue-Dong, Y. Guo, H. Zhang, Electrochem. Commun. 12 (2010) 557–560.
[11] Y. Guo, S. Guo, J. Ren, Y.a.D. Zhai Shaojun, E. Wang, ACS Nano. 4 (2010) 4001–4010.
[12] G. Zhu, P. Gai, L. Wu, J. Zhang, X. Zhang, J. Chen, Chem.—Asian J. 7 (2012) 732–737.
[13] Y. Guo, S. Guo, J. Li, E. Wang, S. Dong, Talanta 84 (2011) 60–64.
[14] Y.J. Guo, Y.H. Chen, Q. Zhao, S.M. Shuang, C. Dong, Electroanalysis 23 (2011) 2400–2407.
[15] Y. Yang, Y. Zhang, Y. Chen, D. Zhao, J. Chen, Y. Liu, Chem.—Eur. J. 18 (2012) 4208–4215.
[16] M. del Pozo, P. Hernandez, L. Hernandez, C. Quintana, J. Mater. Chem. 21 (2011) 13657–13663.
[17] M. del Pozo, E. Blanco, E. Fatás, P. Hernández, C. Quintana, Analyst 137 (2012) 4302–4308.
[18] W.S. Hummers, R.E. Offeman, J. Am. Chem. Soc. 80 (1958) 1339.
[19] V. Carralero, A. Gonzalez Cortes, P. Yanez Sedeno, J. Pingarron, Electroanalysis 17 (2005) 289–297.
[20] M. Sa, L. Ying, T. Ai-Guo, X. Le-Dong, R. Ya-Ping, Clin. Chim. Acta 413 (2012) 973–977.
[21] G. Kuminek, H.K. Stulzer, M.P. Tagliari, P.R. Oliveira, L.S. Bernardi, G.S. Rauber, S.G. Cardos., J. AOAC Int. 94 (2011) 1785–1790.
[22] W.S. Jeon, K. Moon, S.H. Park, H. Chun, Y.H. Ko, J.Y. Lee, E.S. Lee, S. Samal, N.a.R. Selvapalam M.V, V. Sindelar, D. Sobransingh, Y. Inoue, A.E. Kaifer, K. Kim, J. Am. Chem. Soc. 127 (2005) 12984–12989.
[23] W.S. Jeon, H.J. Kim, C. Lee, K. Kim, Chem. Commun. (2002) 1828–1829.
[24] N.G. Shang, P. Papakonstantinou, M.a.C McMullan Ming, A. Stamboulis, A. Potenza, S.S. Dhesi, H. Marchetto, Adv. Funct. Mater. 18 (2008) 3506–3514.
[25] Y. Fan, J.H. Liu, H.T. Lu, Q. Zhang, Microchim. Acta. 173 (2011) 241–247.
[26] V. Sindelar, M.A. Cejas, F.M. Raymo, W.Z. Chen, S.E. Parker, A.E. Kaifer, Chem.—Eur. J 11 (2005) 7054–7059.
[27] M. Bush, N. Bouley, A. Urbach, J. Am. Chem. Soc. 127 (2005) 14511–14517.